

LEO+ & LEO+ Baby

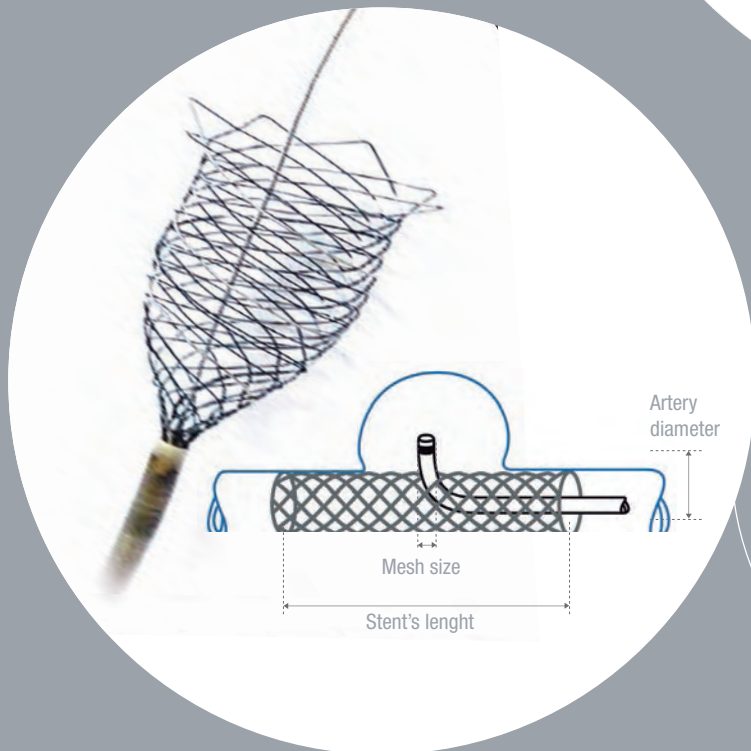
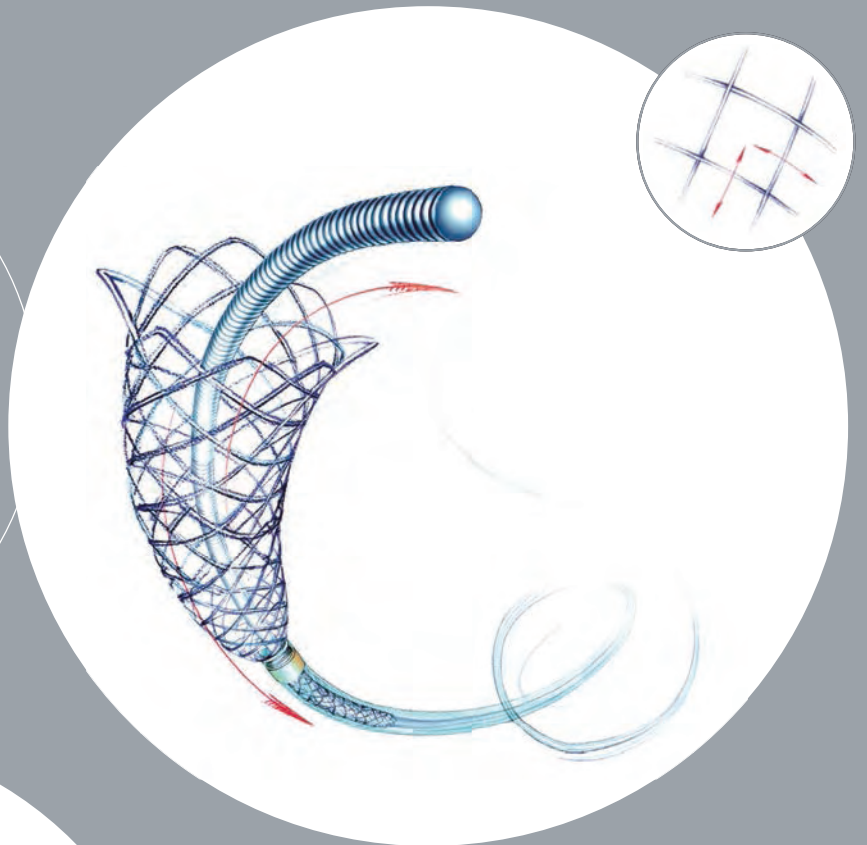
THE ORIGINAL BRAIDED INTRACRANIAL STENTS



LEO+

Self-Expandable LEO+:

- Intracranial stent designed for the treatment of wide-neck aneurysm
- Braided design allows the fine nitinol wires to slide smoothly onto each other to reach perfect vessel conformability, as well as provide coil support



LEO+ Baby

The original braided stent is also compatible with a coiling microcatheter 1 (VASCO+10, ID: .017")

- LOW PROFILE to gain access to vessels down to \varnothing 1,5mm
- Avoid microcatheter exchange



INNOVATION, ANYWAY
www.balt.fr



distributed by

abmedica®

Via Nerviano, 31
20020 Lainate (MI)
tel. +39 02933051
fax +39 0293305400
www.abmedica.it

Emerging Techniques for Evaluation of the Hemodynamics of Intracranial Vascular Pathology

Warren Chang¹, Melissa Huang² and Aichi Chien²

Abstract

Advances in imaging modalities have improved the assessment of intracranial hemodynamics using non-invasive techniques. This review examines new imaging modalities and clinical applications of currently available techniques, describes pathophysiology and future directions in hemodynamic analysis of intracranial stenoses, aneurysms and arteriovenous malformations and explores how hemodynamic analysis may have prognostic value in predicting clinical outcomes and assist in risk stratification. The advent of new technologies such as pseudo-continuous arterial spin labeling, accelerated magnetic resonance angiography (MRA) techniques, 4D digital subtraction angiography, and improvements in clinically available techniques such as phase-contrast MRA may change the landscape of vascular imaging and modify current clinical practice guidelines.

Keywords

magnetic resonance angiography, aneurysms, arteriovenous malformations, stenoses, stroke, intracranial hemorrhage, computational fluid dynamics, hemodynamics, flow

Introduction

The assessment of intracranial flow has long been a challenge because of the numerous challenges inherent in neurovascular imaging. One challenge is the small size of most intracranial structures, which require high spatial resolution in order to acquire adequate measurements. This has limited the modalities that are clinically useful in evaluating intracranial pathologies because of long acquisition time and limited spatial resolution. Also, the solid bone of the cranial vault makes acquisition of images using modalities such as Doppler ultrasound and to some degree, CT/CT angiography (CTA), challenging because of sonic attenuation and/or artifact.

Assessment of neurovascular hemodynamics has clinical utility for several reasons. Evaluation of velocity in intra-arterial stenoses provides functional data that has prognostic value, as shown in the NASCET study in the assessment of the extracranial internal carotid artery.¹ Numerous studies have shown that flow patterns in aneurysms may correlate with clinical outcomes, and in some settings, may have prognostic value.^{2–12} Investigators have also found promising initial results in the use of hemodynamics of arteriovenous malformations for risk stratification.^{13–15} Furthermore, numerous groups have investigated the role of hemodynamics in relation to the role of the endothelium in disease pathophysiology.

New techniques in evaluating intracranial hemodynamics with high spatial resolution within clinically useful imaging times carry promise in the evaluation and treatment of intracranial vascular disease.

To date, evaluation of intracranial hemodynamics has primarily been conducted using digital subtraction angiography (DSA) and computational fluid dynamics (CFD). DSA has long been the gold standard for the evaluation of intracranial pathology.¹⁶ DSA has the highest spatial resolution (~0.1 mm isotropic) and high temporal resolution (30 fps). This allows small lesions such as aneurysms to be completely characterized. DSA also has a large FOV, allowing visualization of large lesions such as arteriovenous malformations (AVMs). Contrast dynamics allows characterization of vessel hemodynamics. Angiography is also both diagnostic and therapeutic, allowing interventions such as angioplasty with stent placement, coiling of aneurysms and embolization of AVMs. However, DSA involves the use of ionizing radiation (up to

¹University of California; Los Angeles, CA, USA

²UCLA Department of Radiology; Los Angeles, CA, USA

Corresponding author:

Warren Chang, MD, MBA, Radiologist, Radiology Department, University of California, Los Angeles, 757 Westwood Plaza, Los Angeles, CA 90095 USA.
Email: warrenchang@mednet.ucla.edu

four times as much as CTA), and iodinated contrast agents, with the risk of contrast-induced nephropathy. Furthermore, DSA carries the risk of catheter-induced iatrogenic stroke, resulting in morbidity and mortality from 1–4%.^{17,18} DSA also requires an experienced operator, typically a neurointerventional radiologist to perform the procedure. Therefore, while DSA is a good modality for the initial evaluation or reassessment of intracranial lesions, staffing issues, radiation exposure and risk of iatrogenic stroke are high and unsuitable for routine follow-up imaging.

Phase-contrast magnetic resonance angiography (PC-MRA) is a non-contrast MRA technique that encodes velocity with the phase of the readout, typically using a bipolar gradient. This allows direct evaluation of the velocity of flow. In the past, phase-contrast MRA has been limited by excessively long scan times and low spatial resolution when compared to DSA, TOF, and CTA. However, recent advances in clinically available pulse sequences have decreased scan time and increased spatial resolution of PC-MRA acquisitions, allowing spatial resolution approaching that of TOF and CTA acquisitions with comprehensive exams in less than ten minutes. Although DSA still has much higher spatial resolution than MRA, the lack of ionizing radiation, iodinated contrast reagents, and non-invasive nature of PC-MRA are attractive. Advances in PC-MRA may allow better evaluation of neurovascular pathology in the near future.

Evaluation of Wall Shear Stress in Neurovascular Pathology

Several techniques such as phase-contrast MRA and CFD images acquired using DSA, CTA or MRA data allow analysis of hemodynamics within stenoses, aneurysms, and AVMs after post-processing. Post-processing allows not only raw hemodynamic parameters such as velocity or secondary parameters such as flow and wall shear stress (WSS) to be calculated, but 3D representations of stenoses, aneurysms and AVMs can be generated with graphical WSS, streamline/particle path, and velocity maps, allowing visual analysis. Figure 1 demonstrates an internal carotid artery aneurysm with elevated WSS at the aneurysm neck and at the impact zone of the inflow jet, also seen on the streamline plot in Figure 2. These figures were generated using CFD from DSA. CFD maps require several hours of processing time per case, while evaluation from 4D PC-MRA requires somewhat less post-processing and can be performed in minutes. Graphical maps allow more intuitive analysis and make it easier to quickly determine patterns that may be relevant to the patient's prognosis.

Intracranial Stenosis

Intracranial stenoses are thought to cause a relatively small but significant portion of ischemic strokes in the

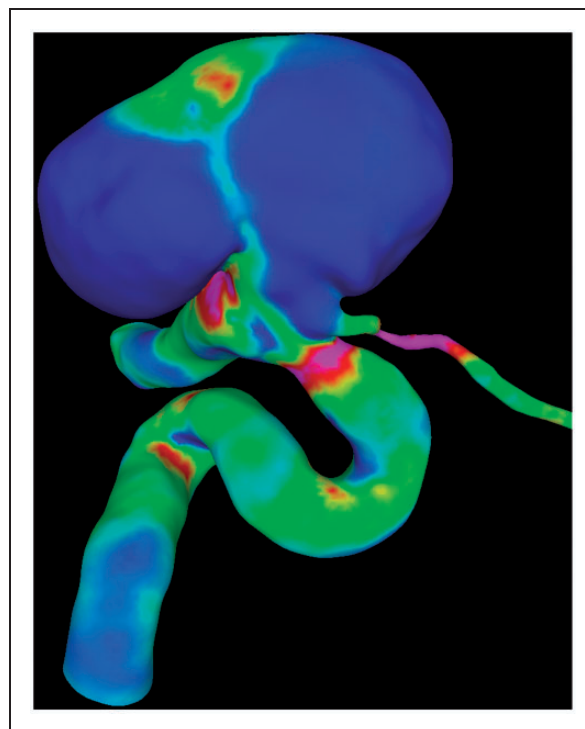


Figure 1. An image generated from computational fluid dynamics from a DSA acquisition showing a wall shear stress (WSS) map of an internal carotid aneurysm demonstrating high levels of WSS at the aneurysm neck and at the impact zone of an inflow jet.

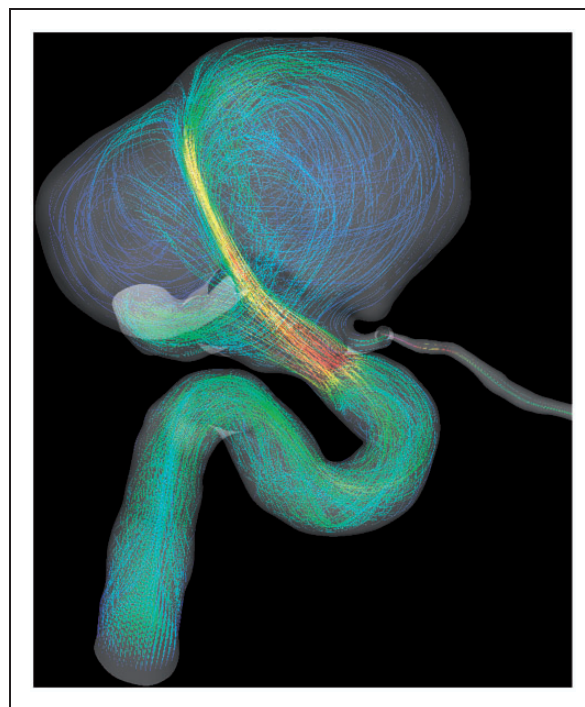


Figure 2. An image from computational fluid dynamics from a DSA acquisition showing streamlines with an internal carotid artery aneurysm demonstrating inflow jet morphology.

Table 1. Summary of standard imaging modalities.

Technique:	Advantages:	Disadvantages:	Indications:
DSA	Highest spatial resolution (0.1 mm voxel size), high temporal resolution, (essentially real time), can be used for both diagnostic and interventional studies. Contrast dynamics give hemodynamic data.	Risk of iatrogenic stroke, invasive, requires arterial catheterization typically with femoral puncture, requires iodinated contrast, exposes patient to ionizing radiation, requires interventionalist present.	Secondary anatomical evaluation/treatment of aneurysms and AVMs.
MRA	Does not require radiation. High spatial resolution for evaluation of arteries with TOF. Adequate spatial resolution with PC-MRA. Does not require iodinated contrast. Phase-contrast MRA has velocity encoding for hemodynamics.	Lower spatial resolution. Gadolinium carries a risk of NSF for patients with renal failure. Lengthy acquisition. Expensive compared to CT. Typically can't be used in patients with pacemakers.	Follow-up anatomical evaluation of intracranial stenoses, aneurysms, and AVMs due to lack of ionizing radiation. PC-MRA be used for hemodynamic analysis for any pathology. Can be used to evaluate vessels as part of a stroke workup.
CFD	Highest spatial resolution for hemodynamic analysis. Excellent hemodynamic data and allows surface-rendered images for intuitive analysis.	Relatively time consuming, may require hours per case, not useful for real time evaluation for a clinical exam, use is confined to research at this time. Typically requires DSA for best results.	Post-processing analysis for hemodynamic assessment of aneurysms, stenoses, and AVMs.
Accelerated MRA	Higher spatial resolution and shorter scan times than standard sequences. Several studies have shown quality of anatomic imaging is clinically comparable to TOF and approaching DSA.	Non-standard sequences, not FDA approved, requires research protocol to use clinically until approval is obtained. May require a trained technologist or researcher to be in the control room to acquire studies.	Research protocols for anatomical assessment of stroke, aneurysms, stenoses, and AVMs.
4D-DSA	Approaches the resolution of DSA without requiring a femoral puncture, can be administered through peripheral IV.	Currently in research state, not FDA approved. No hemodynamic data from intra-arterial contrast dynamics. Lower temporal resolution.	Research protocols until FDA approval is granted for anatomical assessment of AVMs and aneurysms.
PC-ASL	Does not require contrast, can provide both perfusion imaging of the whole brain as well as angiography. No risk of NSF. Can be used as part of a comprehensive stroke examination. Can be combined with PC-MRA for hemodynamics..	Still primarily a research sequence. Questionable efficacy when compared to DSC-MRP on currently available product sequences.	Research protocols for assessment of MR perfusion and MR angiography.

US (~10%), and a much larger portion of ischemic strokes worldwide, up to 50%.¹⁹ Therefore, clinical assessment of stroke and risk assessment would appear to have high clinical utility. Evaluation of intracranial stenosis to date has primarily been limited to anatomic evaluation, most commonly with either DSA or CT angiography. Middle cerebral artery stenoses can be occasionally evaluated with Doppler ultrasound, but this is limited. MRA is occasionally used for anatomic evaluation of stenoses.^{18,20}

The direct routine clinical assessment of flow in stenoses to date has mostly been limited to extracranial structures. Renal artery stenosis (RAS) and carotid

stenosis are the most common stenoses that are evaluated, and they are both evaluated with Doppler ultrasound. RAS is typically evaluated on both waveform (including resistive index) and velocity, whereas evaluation of carotid stenosis is primarily done by velocimetry.¹ However, investigations of global metabolic activity via SPECT or blood flow via MR/CT perfusion has shown hypometabolism and decreased cerebral blood flow in arterial stenoses before the appearance of symptoms or with acetazolamide challenges, allowing assessment of the hemodynamic severity of said stenoses and assessment of collateral reserve.²¹

Hemodynamic assessment of WSS in and around intracranial stenoses may have value in assessing the endothelium and may offer prognostic value in determining the risk of future thromboembolic events.^{22–25} One recent study²⁶ showed that the highest level of WSS is on the surface of a plaque in a high-grade internal carotid stenosis leading to plaque rupture and stroke. A study examining intracranial stenosis using phase-contrast MRA demonstrated increased WSS inside middle cerebral artery stenoses and decreased WSS proximal and distal to the stenosis, as well as increased pressure gradients across the stenosis, when compared to the normal contralateral side.²⁷ The WSS and pressure gradients appeared to correlate with the degree of stenosis. Several studies have shown that low WSS proximal and distal to stenoses leads to the deposition of atherogenic plaque and propagation of stenoses; the mechanism was thought to be secondary to endothelial dysregulation leading to a decrease in vessel caliber,²⁸ increased residence time of arterial blood in the border zones immediately proximal and distal to the stenoses allowing for increased deposition of atherogenic products,²⁹ and turbulent flow, also leading to endothelial dysregulation.^{30,31} Another approach that has recently been adopted is the use of high resolution T1 imaging for the assessment of intraluminal plaque and the endothelium in concert with MRA.³² This technique may have clinical utility in the evaluation of stenoses and other neurovascular pathologies. Therefore, hemodynamic analysis may have prognostic value in determining the risk of ischemic stroke and disease progression in intracranial stenoses. Another recent study noted that signal intensity on TOF-MRA was negatively correlated with infarct volume as seen on diffusion-weighted imaging.³³

Aneurysms

Due to the catastrophic consequences of aneurysmal subarachnoid hemorrhage (50% case fatality rate³⁴), there has long been interest in determining risk factors predisposing patients to aneurysm rupture. Size has long been identified as a risk factor for aneurysm rupture, however, a recent study by Villablanca et al.³⁵ found the most important risk factor for aneurysm rupture was growth, even for aneurysms smaller than the typical 7mm treatment threshold, with smoking and initial size also found to be independent risk factors. Intracranial flow analysis of aneurysms is an active area of investigation, with mixed findings regarding hemodynamic patterns leading to increased growth and rupture. There appears to be two disparate schools of thought regarding hemodynamic conditions that predispose patients towards aneurysm growth and rupture. Several groups have identified elevated focal WSS states and complex/disturbed flow as predisposing patients to aneurysm growth/rupture, while several other groups have identified low WSS as predisposing

patients towards endothelial dysregulation and aneurysm growth/rupture.^{36–48,52–55}

High WSS in Aneurysm Growth and Rupture

Given several new studies demonstrating that growth was the most important single risk factor contributing to aneurysm rupture, evaluating risk factors leading to aneurysm growth has clinical utility. Smoking was a risk factor identified in most studies³⁶ but single aneurysms were noted to have a higher growth rates while multiple aneurysms were more likely to show interval growth.

Multiple studies have examined the role of hemodynamics on aneurysm growth.^{37,38} It is thought that high WSS levels predispose towards the growth of aneurysms,^{39,40} a process that is thought to be secondary to the response of endothelial mechanoreceptors responding to the increased stimulus from high WSS leading to upregulation of inducible nitric oxide synthase (iNOS).^{41,42} Inducible nitric oxide synthase has been shown to lead to regional arterial vasodilatation, ameliorating the effects of elevated WSS, but also thought to be associated with cell injury. Several studies showed that inhibition of nitric oxide synthase in a rat model using a nitric oxide synthase inhibitor decreased the incidence of induced cerebral aneurysms. However, another more recent study,⁴³ illustrating the complexity of endothelial regulatory processes, demonstrated that there are other isoforms of nitric oxide synthase, endothelial, e-NOS, and neuronal, n-NOS, which also work in concert to ameliorate the effects of elevated WSS, and knocking out these two isoforms increased the incidence of induced cerebral aneurysms in a rat model. Regardless of this, all of the studies agreed that elevated WSS led to endothelial damage. Other studies have shown that elevated WSS also leads to upregulation of TGF- β 1, which mediates angiogenesis and VEGF-mediated apoptosis, leading to aneurysm growth. Aneurysms are also shown to demonstrate elevated levels of inflammatory markers including matrix metalloproteases, which may also contribute to endothelial derangement leading to growth.^{44–46} Shojima et al. showed that the aneurysm neck demonstrates the highest levels of WSS, while Rossitti et al. showed that chronic elevated WSS leads to vessel dilatation,^{47,48} which may partially explain the growth patterns of aneurysms.

Several investigators have found that primary inflow jet morphology leading to focally increased WSS to be predisposed to rupture, with helical flow morphology being associated with stability.^{2–5} Figures 1 and 2 demonstrate an internal carotid artery aneurysm with focally increased WSS at the impact zone (Figure 1) and inflow jet morphology seen on the streamline plot (Figure 2). Spatial flow complexity, temporal complexity, and disturbed flow are other risk factors associated with aneurysm rupture; this is also thought to be due to the complex flow causing derangement in endothelial

regulation.^{6–8} Several studies have noted that elevated WSS within the aneurysm sac was more commonly seen in ruptured aneurysms.^{9,10} Several other studies have noticed that increased pulsatility in aneurysms tends to increase the risk of rupture, possibly secondary to transient changes in WSS.^{11,12} Another study has demonstrated that sudden increases in heart rate and blood pressure, which increases WSS, or other factors that change WSS can also play a role, depending on vessel morphology and behaviors that increase these hemodynamic parameters, such as drug use or smoking, are also risk factors for aneurysm growth and rupture.⁴⁹ Aneurysm morphology has also been associated with rupture risk;^{50,51} most ruptured aneurysms demonstrated a ratio of aneurysmal volume to bounding sphere between 0.5 and 1.0.

Low WSS in Aneurysm Growth/Rupture

While several studies have found a trend of high WSS and inflow jet morphology in ruptured aneurysms, another group of studies found that low WSS states are often found in ruptured aneurysms and lead to growth, thrombosis, and eventual rupture.^{37,48,52–55} These studies hypothesize that a certain level of WSS is needed to maintain the endothelium, and low WSS states lead to endothelial apoptosis, aneurysm expansion, and rupture. That said, most groups do acknowledge that the inflow jet morphology and elevated WSS leading to initial aneurysm growth² may be an early finding in aneurysms while the later low WSS state is an adaptation in later stages of aneurysm development, or that high WSS states could be a different pathway to aneurysm rupture.

Arteriovenous Malformations

Like aneurysms, AVMs have been an active area of investigation because of the risk of hemorrhage. While hemorrhage from an AVM typically is not as catastrophic as subarachnoid hemorrhage from a ruptured cerebral aneurysm, the risk of bleeding from an AVM tends to be higher than that of cerebral aneurysm rupture. Furthermore, treatment of AVMs, depending on the Spetzler-Martin grade, often carries higher mortality and morbidity than treatment of cerebral aneurysms, especially after the advent of effective endovascular techniques. Therefore, stratification of patients into groups with differing risk of hemorrhage has high clinical utility. AVMs are routinely assessed initially by non-contrast head CT, followed typically by CTA for further characterization. DSA is also used at times, especially when impending endovascular treatment is likely. Routine follow-up imaging of AVMs is typically done via MRI and TOF-MRA.

Numerous studies have studied risk factors for hemorrhage based on demographics and clinical factors^{56,57} and the most significant risk factor for future

hemorrhagic events was found to be prior hemorrhage. Deep brain location and deep venous drainage were other significant risk factors, and the annual risk of hemorrhage ranged from 1–34% depending on the absence or presence of these risk factors. The ARUBA trial examined the outcomes of treatable AVMs with and without treatment, and found that event rates in the treatment group were more than three times higher than in the non-treatment group; indeed, enrollment in the trial was halted due to a very high rate of adverse events in the treatment arm.⁵⁸ However, many argue that this analysis is incomplete for several reasons. First, and most notably, the follow-up period for the study was 33 months, and one would expect the majority of adverse events in the treatment group to occur near the time of intervention, whereas adverse events from the untreated AVM can occur at any point during the patients' lives. Also, the incidence of morbidity of intervention used to end the trial seems to be higher than what has been found by several large trials.⁵⁹ That said, individual risk stratification of hemorrhagic risk if possible would have high clinical utility due to the high potential morbidity from intervention, which included 5.1–7.4% risk of death, symptomatic stroke, or significant neurologic impairment in a large meta-analysis⁶⁰ and the high variability of annual hemorrhage risk as described above.

Analysis of flow in intracranial AVMs is an active area of investigation, and several groups have reported promising results to date. The endothelial factors described above regarding the pathogenesis of aneurysms also apply in AVMs. Due to the lack of a functional intervening capillary bed, AVMs demonstrate very high flow, and thus, significantly elevated WSS relative to normal patients. This elevated WSS leads to endothelial adaptation and the upregulation of nitric oxide synthase isotypes as well as other pro-angiogenic and pro-inflammatory factors. One adaptation seen in AVMs is compensatory arterial vasodilatation. One study found that high WSS values led to statistically significant compensatory vasodilation in feeding arteries in patients with a more stable clinical presentation where patients presenting with acute hemorrhage did not have the same degree of vasodilatation in arterial feeders. This suggests that this compensatory mechanism may be protective and failure to compensate for large changes in flow may be pathogenic.¹³ Several other studies found that AVM hemodynamics do not necessarily correlate with their Spetzler-Martin grade and in many cases their abnormal hemodynamics revert towards normal after staged embolization.^{14,15} Young et al.⁵⁷ examined the role of the endothelium in AVM growth and proliferation and found that endothelial changes and gene expression are altered in AVMs, also suggesting that abnormal WSS causing endothelial derangement may play a role in the pathophysiology of AVMs.

New Techniques

Several new techniques have emerged recently that may help advance the state of anatomic and flow imaging and quantification.

4D digital subtraction angiography (4D-DSA) is a recent advance in DSA developed by researchers at the University of Wisconsin which uses projection reconstruction to reconstruct time-resolved DSA images by using a single 3D-DSA vascular volume as a constraining image and acquiring a series of projections before and after an intravenous contrast injection.^{61,62} This allows the creation of a time-resolved series with better spatial resolution than CTA/MRA but improved small vessel contrast due to the availability of a maximum intensity projection. Allowing the acquisition of high-resolution angiograms with a peripheral intravenous injection greatly decreases the complication rate from DSA as well as decreasing the amount of radiation and contrast needed. This technique appears promising but further investigation will be required prior to large scale implementation. Due to the intravenous rather than intra-arterial contrast injection, 4D-DSA does not have the same contrast dynamics for direct perfusion analysis that 3D-DSA does, so it is less effective for hemodynamic analysis of lesions, but does offer improved safety compared to 2D/3D-DSA. Another option is the use of advanced reconstruction techniques with 2D-DSA which may also provide additional hemodynamic analysis through the use of contrast dynamics. A recent study investigating the use of 2D-DSA for hemodynamic analysis with patients with pipeline stents and flow diverters showed that the technique offers additional options for patients in which DSA is the primary method for analysis.⁶³

Accelerated MRA

Numerous groups have developed accelerated PC-MRA techniques which have increased spatial resolution while decreasing acquisition time in MRA. Techniques such as parallel imaging, view-sharing, and generalized autocalibrating partially parallel acquisition, have greatly improved the performance of traditional Cartesian 3D/4D acquisitions. Radial or partially radial MRA techniques such as phase contrast vastly undersampled projection reconstruction⁶⁴ and phase contrast stack of stars (PC-SOS)⁶⁵ have improved the spatial resolution of whole-brain and limited brain scans while decreasing scan time. PC-SOS allows in-plane resolution to equal that of 3D-TOF and CTA while maintaining sub/peri-centimeter out of plane resolution. Advanced MRA often leverage the inherent sparsity present in neurovascular imaging to enhance the resolution and speed of acquisitions. These sequences tend to demonstrate higher spatial resolution with lower acquisition time. Another possibility is to combine a low resolution time-resolved series of contrast MR examinations with a longer phase-contrast acquisition to obtain a composite series with

both high temporal and spatial resolution^{66,67} which offer venous and arterial assessment of AVMs of diagnostic quality. However most current accelerated MRA techniques are not yet “plug-and-play” and require a medical physicist or specially trained technician to acquire the images. However, advances in MRA research translate to clinically available sequences and several accelerated MRA sequences may be clinically available on scanners soon. Many MRA techniques use post-processing software with either accelerated MRA techniques or clinically available MRA sequences.^{68–70} This approach allows examinations to be acquired as part of the normal clinical workflow. Several studies have compared the assessment of areas of complex flow in both advanced and clinical 4D-MRA sequences using automated post-processing tools to that using CFD and have found similar results.^{27,71}

ASL/PCASL

ASL is a technique used for perfusion imaging that is capable of acquiring whole-brain perfusion imaging without the use of exogenous contrast agents. Clinically available product sequences using ASL have begun being introduced, and initial results appear promising.^{72,73} Pseudo-continuous arterial spin labeling (PC-ASL) is a technique that greatly enhances the speed of ASL acquisitions by using a train of discrete RF pulses to mimic continuous tagging, improving clinical utility.

PC-ASL cannot only be used for brain perfusion imaging but can also be used for angiography. The contrast differences between spin labeled vessels and brain parenchyma seen in ASL, combined with the sparsity inherent in neurovascular imaging make PC-ASL a promising technique for intracranial neurovascular imaging. Several groups have investigated the use of PC-ASL in 4D-MRA. Wu et al. examined the use of PC-ASL with an accelerated 3D radial angiography technique and found that PC-ASL has utility in evaluating high-flow structures such as AVMs and also provides hemodynamic information such as arrival times. Using a phase-contrast technique with PC-ASL will also provide velocity information.^{74,75} This may be of clinical utility as part of a comprehensive stroke examination.

Conclusions

This report examines the current state of hemodynamic assessment of intracranial vessels, describes current research into the applications of intracranial flow, and explores several emerging techniques that may advance the field of intracranial flow. Given the high global clinical burden of ischemic stroke in the setting of atherosclerosis and high morbidity and mortality seen in aneurysm and AVM rupture, techniques that may offer prognostic information regarding these pathologic

states have high clinical utility. The ideal technique for evaluation of these pathologies outside the emergency setting would have high spatial resolution, clinically useful scan times, and low mortality/morbidity. Recent advances in MRA have improved its clinical efficacy. Although MRA still offers inferior spatial resolution to CTA/DSA for anatomic detail and CFD for hemodynamic assessment, recent studies have noted similar results in examinations of AVMs and aneurysms. Further advances in technology may continue to enhance the viability of MRA.

Funding

This research received no specific grant from any funding agency in the public, commercial or not-for-profit sectors.

Conflict of interest

The authors declare no conflict of interest.

References

- Ferguson G, Eliasziw M, Barr H, et al. The North American Symptomatic Carotid Endarterectomy Trial. *Stroke* 1999; 30: 1751–1758.
- Hope T, Hope M, Purcell D, et al. Evaluation of intracranial stenoses and aneurysms with accelerated 4D flow. *Magn Reson Imaging* 2010; 28: 41–46. doi: 10.1016/j.mri.2009.05.042.
- Cebral J, Mut F, Weir J, et al. Quantitative characterization of the hemodynamic environment in ruptured and unruptured brain aneurysms. *Am J Neuroradiol* 2011; 32: 145–151.
- Cebral J, Mut F, Weir J, et al. Association of hemodynamic characteristics and cerebral aneurysm rupture. *Am J Neuroradiol* 2011; 32: 264–270. doi: 10.3174/ajnr.A2274.
- Sforza D, Putman C, Scrivano E, et al. Blood-flow characteristics in a terminal basilar tip aneurysm prior to its fatal rupture. *Am J Neuroradiol* 2010; 31: 1127–1131. doi: 10.3174/ajnr.A2021.
- Byrne G, Mut F and Cebral J. Quantifying the large-scale hemodynamics of intracranial aneurysms. *Am J Neuroradiol* 2014; 35: 333–338. doi: 10.3174/ajnr.A3678.
- Mut F, Löhner R, Chien A, et al. Computational hemodynamics framework for the analysis of cerebral aneurysms. *Int J Numer Method Biomed Eng* 2011; 27: 822–839. doi: 10.1002/cnm.1424.
- Xiang J, Natarajan S, Tremmel M, et al. Hemodynamic-morphologic discriminants for intracranial aneurysm rupture. *Stroke* 2011; 42: 144–152.
- Chien A, Tatshima S, Castro M, et al. Patient-specific flow analysis of brain aneurysms at a single location: comparison of hemodynamic characteristics in small aneurysms. *Med Biol Eng Comput* 2008; 46: 1113–1120. doi: 10.1007/s11517-008-0400-5.
- Chien A, Tatshima S, Sayre J, et al. Patient-specific hemodynamic analysis of small internal carotid artery-ophthalmic artery aneurysms. *Surg Neurol* 2009; 72: 444–450. doi: 10.1016/j.surneu.2008.12.013.
- Chien A, Sayre J and Viñuela F. Quantitative comparison of the dynamic flow waveform changes in 12 ruptured and 29 unruptured ICA-ophthalmic artery aneurysms. *Neuroradiology* 2013; 55: 313–320. doi: 10.1007/s00234-012-1108-7.
- Patti J, Viñuela F and Chien A. Distinct trends of pulsatility found at the necks of ruptured and unruptured aneurysms. *J Neurointerv Surg* 2014; 6: 103–107. doi: 10.1136/neurintsurg-2013-010660.
- Chang W, Loecher M, Wu Y, et al. Hemodynamic changes in patients with arteriovenous malformations assessed using high-resolution 3D radial phase-contrast MR angiography. *Am J Neuroradiol* 2012; 33(8): 1565–1572. doi: 10.3174/ajnr.A3010.
- Markl M, Wu C, Hurley M, et al. Cerebral arteriovenous malformation: complex 3D hemodynamics and 3D blood flow alterations during staged embolization. *J Magn Reson Imaging* 2013; 38: 946–950. doi: 10.1002/jmri.24261.
- Ansari S, Schnell S, Carroll T, et al. Intracranial 4D flow MRI: toward individualized assessment of arteriovenous malformation hemodynamics and treatment-induced changes. *Am J Neuroradiol* 2013; 34: 1922–1928. doi: 10.3174/ajnr.A3537.
- Crummy A, Steighorst M, Turski P, et al. Digital subtraction angiography: current status and use of intra-arterial injection. *Radiology* 1982; 145: 303–307. doi: 10.1148/radiology.145.2.6753013.
- Hankey GJ, Warlow CP and Molyneux AJ. Complications of cerebral angiography for patients with mild carotid territory ischaemia being considered for carotid endarterectomy. *J Neurol Neurosurg Psychiatry* 1990; 53: 542–548. doi: 10.1136/jnnp.53.7.542.
- Manninen A, Isokangas J, Karttunen A, et al. A comparison of radiation exposure between diagnostic CTA and DSA examinations of cerebral and cervicocerebral vessels. *Am J Neuroradiol* 2012; 33: 2038–2042. doi: 10.3174/ajnr.A3123.
- Wong L. Global burden of intracranial atherosclerosis. *Int J Stroke* 2006; 1(3): 158–159. doi: 10.1111/j.1747-4949.2006.00045.x.
- van Laar P, van der Grond J, Mali W, et al. Magnetic resonance evaluation of the cerebral circulation in obstructive arterial disease. *Cerebrovasc Dis* 2006; 21: 297–306. doi: 10.1159/000091534.
- Tomura N, Otani T, Koga M, et al. Correlation between severity of carotid stenosis and vascular reserve measured by acetazolamide brain perfusion single photon emission computed tomography. *J Stroke Cerebrovasc Dis* 2013; 22(2): 166–170. doi: 10.1016/j.jstrokecerebrovasdis.2011.07.011.
- Leng X, Scalzo F, Lung H, et al. Computational fluid dynamics modeling of symptomatic intracranial atherosclerosis may predict risk of stroke recurrence. *PLoS One* 2014; 9: e97531. doi: 10.1371/journal.pone.0097531.
- Kasner S, Chimowitz M, Lynn M, et al. Predictors of ischemic stroke in the territory of a symptomatic intracranial arterial stenosis. *Circulation* 2006; 113: 555–563. doi: 10.1161/CIRCULATIONAHA.105.578229.
- Liebeskind D, Kosinski A, Lynn M, et al. Noninvasive fractional flow on MRA predicts stroke risk of intracranial stenosis. *J Neuroimaging* 2014; 5: 87–91. doi: 10.1111/jon.12101.
- Schirmer C and Malek A. Estimation of wall shear stress dynamic fluctuations in intracranial atherosclerotic lesions using computational fluid dynamics.

- Neurosurgery* 2008; 63: 326–335. doi: 10.1227/01.NEU.0000313119.73941.9E.
26. Suh D, Park S, Oh T, et al. High shear stress at the surface of enhancing plaque in the systolic phase is related to the symptom presentation of severe M1 stenosis. *Korean J Radiol* 2011; 12: 515–518. doi: 10.3348/kjr.2011.12.4.515.
 27. Chang W, Loecher M, Johnson K, et al. Calculation of relative pressure and wall shear stress gradients. In: Intracranial arterial stenoses using high-resolution 3D-radial phase contrast velocimetry (PC-VIPR). Presented at the 97th Annual Meeting of the Radiological Society of North America, Chicago, IL, 11/27-12/2. 2011.
 28. Malek A, Alper S and Izumo S. Hemodynamic shear stress and its role in atherosclerosis. *JAMA* 1999; 282: 2035–2042. doi: 10.1001/jama.282.21.2035.
 29. Glagov S, Zarins C, Giddens DP, et al. Hemodynamics and atherosclerosis: insights and perspectives gained from studies of human arteries. *Arch Pathol Lab Med* 1988; 112: 1018–1031.
 30. Chiu J and Chien S. Effects of Disturbed Flow on Vascular Endothelium: Pathophysiological Basis and Clinical Perspectives. *Physiological Reviews* 2011; 91: 327–387. doi: 10.1152/physrev.00047.2009.
 31. Gimbrone Jr, MA, Topper JN, Nagel T, et al. Endothelial dysfunction, hemodynamic forces, and atherogenesis. *Ann NY Acad Sci* 2000; 902: 230–240. doi: 10.1111/j.1749-6632.2000.tb06318.x.
 32. Qiao Y, Etesami M, Malhotra S, et al. Identification of intraplaque hemorrhage on MR angiography images: a comparison of contrast-enhanced mask and time-of-flight techniques. *Am J Neuroradiol* 2011; 32: 454–459. doi: 10.3174/ajnr.A2320.
 33. Leng X, Wong K, Soo Y, et al. Magnetic resonance angiography signal intensity as a marker of hemodynamic impairment in intracranial arterial stenosis. *PLoS ONE* 2013; 8: e80124. doi: 10.1371/journal.pone.0080124.
 34. van Gijn J and Rinkel G. Subarachnoid haemorrhage: diagnosis, causes and management. *Brain* 2001; 124: 249–278. doi: 10.1093/brain/124.2.249.
 35. Villablanca J, Duckwiler G, Jahan R, et al. Natural history of asymptomatic unruptured cerebral aneurysms evaluated at CT angiography: growth and rupture incidence and correlation with epidemiologic risk factors. *Radiology* 2013; 269: 258–265. doi: 10.1148/radiol.13121188.
 36. Chien A, Liang F, Sayre J, et al. Enlargement of small, asymptomatic, unruptured intracranial aneurysms in patients with no history of subarachnoid hemorrhage: the different factors related to the growth of single and multiple aneurysms. *J Neurosurg* 2013; 119: 190–197. doi: 10.3171/2013.3.JNS121469.
 37. Penn D, Komotar R and Connolly E. Hemodynamic mechanisms underlying cerebral aneurysm pathogenesis. *J Clin Neurosci* 2011; 18: 1435–1438. doi: 10.1016/j.jocn.2011.05.001.
 38. Cebral J and Raschi M. Suggested connections between risk factors of intracranial aneurysms: a review. *Ann Biomed Eng* 2013; 41(7): 1366–1383. doi: 10.1007/s10439-012-0723-0.
 39. Metaxa E, Tremmel S, Natarajan J, et al. Characterization of critical hemodynamics contributing to aneurysmal remodeling at the basilar terminus in a rabbit model. *Stroke* 2010; 41: 1774–1782. doi: 10.1161/STROKEAHA.110.585992.
 40. Meng H, Wang Z, Hoi Y, et al. Complex hemodynamics at the apex of an arterial bifurcation induces vascular remodeling resembling cerebral aneurysm initiation. *Stroke* 2007; 38: 1924–1931. doi: 10.1161/STROKEAHA.106.481234.
 41. Fukuda S, et al. Prevention of rat cerebral aneurysm formation by inhibition of nitric oxide synthase. *Circulation* 2000; 101: 2532–2538. doi: 10.1161/01.CIR.101.21.2532.
 42. Sadamasa N, Nozaki K, Hashimoto N, et al. Disruption of gene for inducible nitric oxide synthase reduces progression of cerebral aneurysms. *Stroke* 2003; 34: 2980–2984. doi: 10.1161/01.STR.0000102556.55600.3B.
 43. Aoki T, Nishimura M, Kataoka H, et al. Complementary inhibition of cerebral aneurysm formation by eNOS and nNOS. *Laboratory Investigation* 2011; 91: 619–626. doi: 10.1038/labinvest.2010.204.
 44. Ohno M, Cooke J, Dzau V, et al. Fluid shear stress induces endothelial transforming growth factor beta-1 transcription and production. *Modulation by potassium channel blockade J Clin Invest* 1995; 95: 1363–1369. doi: 10.1172/JCI117787.
 45. Ferrari G, Cook B, Terushkin V, et al. Transforming growth factor-beta 1 (TGF-beta1) induces angiogenesis through vascular endothelial growth factor (VEGF)-mediated apoptosis. *J Cell Physiol* 2009; 219: 449–458. doi: 10.1002/jcp.21706.
 46. Hashimoto T, Meng H and Young WL. Intracranial aneurysms: links among inflammation, hemodynamics and vascular remodeling. *Neurol Res* 2006; 28: 372–380. doi: 10.1179/016164106X14973.
 47. Rossitti S, Svendsen P, et al. Shear stress in cerebral arteries supplying arteriovenous malformations. *Acta Neurochir (Wien)* 1995; 137(3–4): 138–145, discussion 145. doi: 10.1007/BF02187185.
 48. Shojima M, Oshima M, Takagi K, et al. Computational fluid dynamic study of 20 middle cerebral artery aneurysms. *Stroke* 2004; 35: 2500–2505. doi: 10.1161/01.STR.0000144648.89172.0f.
 49. Jiang J and Strother CM. Computational fluid dynamics simulations of intracranial aneurysms at varying heart rates: a “patient-specific” study. *J Biomech Eng* 2009; 131: 91–101.
 50. Chien A, Sayre J and Viñuela F. Comparative morphological analysis of the geometry of ruptured and unruptured aneurysms. *Neurosurgery* 2011; 69: 349–356. doi: 10.1227/NEU.0b013e31821661c3.
 51. Chien A and Sayre J. Morphologic and hemodynamic risk factors in ruptured aneurysms imaged before and after rupture. *Am J Neuroradiol* 2014; 35(11): 2130–2135. doi: 10.3174/ajnr.A4016.
 52. Rayz V, Bousset L, Lawton M, et al. Numerical modeling of the flow in intracranial aneurysms: prediction of regions prone to thrombus formation. *Ann Biomed Eng* 2008; 11: 1793–804. doi: 10.1007/s10439-008-9561-5.
 53. Bousset L, Rayz V, McCulloch C, et al. Aneurysm growth occurs at region of low wall shear stress: patient-specific correlation of hemodynamics and growth in a longitudinal study. *Stroke* 2008; 39: 2997–3002. doi: 10.1161/STROKEAHA.108.521617.
 54. Raschi M, Mut F, Byrne G, et al. CFD and PIV Analysis of hemodynamics in a growing intracranial aneurysm.

- Int J Numer Method Biomed Eng* 2012; 28(2): 214–228. doi: 10.1002/cnm.1459.
55. Jou L, Wong G, Dispensa B, et al. Correlation between luminal geometry changes and hemodynamics in fusiform intracranial aneurysms. *Am J Neuroradiol* 2005; 26: 2357–2363.
 56. Stapf C, Mast H, Sciacca R, et al. Predictors of hemorrhage in patients with untreated brain arteriovenous malformation. *Neurology* 2006; 66: 1350–1355. doi: 10.1212/01.wnl.0000210524.68507.87.
 57. Young WL. Arteriovenous malformations clinical and genetic risk stratification. Presented at the 49th Annual Meeting of the American Society of Neuroradiology, Seattle, Washington, 6/4-6/9. 2011.
 58. Mohr J, Parides M, Stapf C, et al. Medical management with or without interventional therapy for unruptured brain arteriovenous malformations (ARUBA): a multicentre, non-blinded, randomised trial. *Lancet* 2014; 383: 614–621. doi: 10.1016/S0140-6736(13)62302-8.
 59. Russin J and Spetzler R. Commentary: The ARUBA trial. *Neurosurgery* 2014; 75(1): E96–97. doi: 10.1227/NEU.0000000000000357.
 60. van Beijnum J, van der Worp HB, Buis DR, et al. Treatment of brain arteriovenous malformations: a systematic review and meta-analysis. *JAMA* 2011; 306: 2011–2019. doi: 10.1001/jama.2011.1632.
 61. Grist T, Mistretta C, Strother C, et al. Time-resolved angiography: Past, present, and future. *J Magn Reson Imaging* 2012; 36: 1273–1286. doi: 10.1002/jmri.23646.
 62. Davis B, Royalty K, Kowarschik M, et al. 4D digital subtraction angiography: implementation and demonstration of feasibility. *Am J Neuroradiol* 2013; 34: 1914–1921. doi: 10.3174/ajnr.A3529.
 63. Chien A and Viñuela F. IS FlowMap, a novel tool to examine blood flow changes induced by flow diverter stent treatment: initial experiences with pipeline cases. *J Neurointerv Surg* 2013; 5: 43–47. doi: 10.1136/neurintsurg-2012-010613.
 64. Johnson K, Lum D, Turski P, et al. Improved 3D phase contrast MRI with off-resonance corrected dual echo VIPR. *Magn Reson Med* 2008; 60: 1329–1336. doi: 10.1002/mrm.21763.
 65. Kecskemeti S, Johnson K, Wu Y, et al. High resolution three-dimensional cine phase contrast MRI of small intracranial aneurysms using a stack of stars k-space trajectory. *J Magn Reson Imaging* 2012; 35: 518–527. doi: 10.1002/jmri.23548.
 66. Velikina J, Johnson K, Wu Y, et al. PC HYPR flow: a technique for rapid imaging of contrast dynamics. *J Magn Reson Imaging* 2010; 31: 447–456. doi: 10.1002/jmri.22035.
 67. Wu Y, Chang W, Johnson K, et al. Fast whole-brain 4D contrast-enhanced MR angiography with velocity encoding using undersampled radial acquisition and highly constrained projection reconstruction: image-quality assessment in volunteer subjects. *Am J Neuroradiol* 2011; 32: E47–E50. doi: 10.3174/ajnr.A2048.
 68. Markl M, Wallis W and Harloff A. Reproducibility of flow and wall shear stress analysis using flow-sensitive four-dimensional MRI. *J Magn Reson Imaging* 2011; 33: 988–994. doi: 10.1002/jmri.22519.
 69. Chang W, Frydrychowicz A, Kecskemeti S, et al. The effect of spatial resolution on wall shear stress measurements acquired using radial phase contrast magnetic resonance angiography in the middle cerebral arteries of healthy volunteers. *Neuroradiol J* 2011; 24: 115–120.
 70. Chang W, Landgraf B, Johnson K, et al. Velocity measurements in the middle cerebral arteries of healthy volunteers using 3D radial phase-contrast HYPRFlow: comparison with transcranial doppler sonography and 2D phase-contrast MR imaging. *Am J Neuroradiol* 2011; 32: 54–59.
 71. Cebra J, Putman C, Alley M, et al. Hemodynamics in normal cerebral arteries: qualitative comparison of 4d phase-contrast magnetic resonance and image-based computational fluid dynamics. *J Eng Math* 2009; 64: 367–378. doi: 10.1007/s10665-009-9266-2.
 72. Mirasol R, Bokkers R, Hernandez D, et al. Assessing reperfusion with whole-brain arterial spin labeling: a non-invasive alternative to gadolinium. *Stroke* 2014; 45: 456–461. doi: 10.1161/STROKEAHA.113.004001.
 73. Nael K, Meshksar A, Liebeskind D, et al. Quantitative analysis of hypoperfusion in acute stroke: arterial spin labeling versus dynamic susceptibility contrast. *Stroke* 2013; 44: 3090–3096. doi: 10.1161/STROKEAHA.113.002377.
 74. Wu W, Fernández-Seara M and Detre J. A theoretical and experimental investigation of the tagging efficiency of pseudocontinuous arterial spin labeling. *Magn Reson Med* 2007; 58: 1020–1027. doi: 10.1002/mrm.21403.
 75. Wu H, Block W and Turski P. Noncontrast dynamic 3D intracranial MR angiography using pseudo-continuous arterial spin labeling (PCASL) and accelerated 3D radial acquisition. *J Magn Reson Imaging* 2014; 39: 1320–1326. doi: 10.1002/jmri.24279.